KAPL-P-000123
(K98165)

PHASE STABILITY IN $Ga_xIn_{(1-x)}AsySb_{(1-y)}$/GaSb HETEROSTRUCTURES

CONF-981055--

Y. Chen, G. Charache

October 1998

DISTRIBUTION OF THIS DOCUMENT IS UNLIMITED

MASTER

NOTICE

This report was prepared as an account of work sponsored by the United States Government. Neither the United States, nor the United States Department of Energy, nor any of their employees, nor any of their contractors, subcontractors, or their employees, makes any warranty, express or implied, or assumes any legal liability or responsibility for the accuracy, completeness or usefulness of any information, apparatus, product or process disclosed, or represents that its use would not infringe privately owned rights.

KAPL ATOMIC POWER LABORATORY SCHENECTADY, NEW YORK 12301

Operated for the U. S. Department of Energy
by KAPL, Inc. a Lockheed Martin company

DISCLAIMER

This report was prepared as an account of work sponsored by an agency of the United States Government. Neither the United States Government nor any agency thereof, nor any of their employees, makes any warranty, express or implied, or assumes any legal liability or responsibility for the accuracy, completeness, or usefulness of any information, apparatus, product, or process disclosed, or represents that its use would not infringe privately owned rights. Reference herein to any specific commercial product, process, or service by trade name, trademark, manufacturer, or otherwise does not necessarily constitute or imply its endorsement, recommendation, or favoring by the United States Government or any agency thereof. The views and opinions of authors expressed herein do not necessarily state or reflect those of the United States Government or any agency thereof.

DISCLAIMER

Portions of this document may be illegible in electronic image products. Images are produced from the best available original document.

REPRODUCED AT GOV'T EXPENSE

PHASE STABILITY IN $Ga_x In_{(1-x)}As_ySb_{(1-y)}$/GaSb HETEROSTRUCTURES

Y-C.Chen[1], V. Bucklen[1], M.Freeman[2], R.P.Cardines Jr[2],
G. Nichols[2], P. Sanders[2], G. Charache[2], and K. Rajan[1]

[1]Department of Materials Science and Engineering
Rensselaer Polytechnic Institute
Troy, NY 12180-3590
and
[2]Lockheed-Martin, Inc.
Schenectady, NY 12301-1072

ABSTRACT

The crystallographic and microstructural characteristics of liquid phase epitaxy lattice-matched $In_xGa_{(1-x)}As_ySb_{(1-y)}$/GaSb (100) heterostructures is presented. Using both transmission electron microscopy and high resolution X-ray diffraction, a variety of diffusional based phase transformations in the epitaxial films are observed, including: spinodal decomposition, compositional modulations of the order of 30 nm, and weak long range ordering. These results are interpreted in terms of the possible influence of substrate surface structure on the phase stability of epitaxial layers.

INTRODUCTION

The application of III-V compound semiconductor materials in device structures is important for high-speed microelectronics and optoelectronics. These materials have allowed the device engineer to tailor material parameters such as the bandgap and carrier mobility to the need of the device by altering their composition. When using the ternary or quaternary materials, the device designer usually presumes that the compound is completely disordered, without any correlation between the atoms on the sublattices. However, the thermodynamics of the compound often produce material that has some degree of macroscopic or microscopic ordering. Control of such ordering can be used as an additional procedure to tune the optoelectronic properties to specific values for particular devices. Lack of control could result in devices with, for example, emission wavelengths significantly different from the designed values.

Composition modulation is a subset of phase separation [1] and it is often referred to as the spontaneous formation of a phase-separated, self-organized periodic structure. Composition modulation in epitaxial growth has been observed to occur either parallel [2-4] (vertical modulation), perpendicular [5,6] (lateral modulation), or both parallel and perpendicular [4,7] to the growth direction. Recently, there has been a great impetus to apply low dimensional structures to novel electronic and photonic devices [8]. For example, lasers with quantum wire (QWR) active regions are predicted to have lower threshold currents, wider modulation bandwidths, and better temperature stability [8] than conventional two-dimensional quantum well devices. Deposition of short period superlattices (SPS) of some devices by molecular beam epitaxy [9,10] has been shown to result in lateral composition modulation, which has been exploited to obtain high densities of nanometer-sized QWR,

REPRODUCED AT GOVT EXPENSE #49

without the processing limitations of other fabrication methods. Application of this technique to the InAlAs system [8], can lead to novel polarization-sensitive devices. In a laser structure, cladding layers consisting of AlAs/InAs SPS can produce QWR behavior in active layers of InGaAs due to composition-modulation induced strain fields [11].

Compound semiconductor materials have been widely applied to various electronic and optoelectronic devices. Since the microstructure of such materials is an important factor that influences the optoelectronic properies, it is quite important to examine the epilayers microscopically. This paper presents the evolution of weak ordering, composition modulation, microstructure and phase stability of the GaInAsSb system, grown by liquid phase epitaxy (LPE). A variety of experimental techniques are used including: high resolution X-ray diffraction (HRXRD), reciprocal space mapping (RSM), and transmission electron microscopy (TEM). It is expected that similar observations will also be present using other growth techniques such as metalorganic vapor phase epitaxy (MOVPE) or molecular beam epitaxy (MBE).

EXPERIMENTAL DETAILS

The growth parameter space used in this study involved independently examining the effects of epilayer chemistry and the role of substrate misorientation. A series of three different liquid compositions were grown by liquid phase epitaxy. The choice of InGaAsSb composition was dictated by the requirement of achieving a ~0.55 eV bandgap material lattice-matched to GaSb, while remaining in a single-phase region (i.e., outside the spinodal boundary, Figure 1). Hence, three compositions were studied which followed the iso-lattice parameter line associated with lattice matched heterostructures [Fig. 1], and were outside the equilibrium 600°C spinodal boundary [12]. The samples were $Ga_{0.82}In_{0.18}As_{0.14}Sb_{0.86}$ (sample A), $Ga_{0.87}In_{0.13}As_{0.12}Sb_{0.88}$ (sample B), and $Ga_{0.92}In_{0.08}As_{0.07}Sb_{0.93}$ (sample C) grown on GaSb (001) substrates. In order to study the influence of substrate misorientation on phase stability, two additional samples with the same composition as A (close to the equilibrium spinodal boundary) were also studied: sample D (2° misoriented toward <110>) and sample E (2° misoriented toward $<111_B>$).

A conventional horizontal source-seed graphite sliding-boat in a Pd -diffused hydrogen atmosphere was used for the LPE process and the epilayers were grown on commercial Te-doped GaSb wafers. After preparation of the melts and substrate cleaning by a HF acid etch, the solution was remelted at 560 °C for 1 hour followed by a slow ramp to the liquidus temperature of 532 °C. The growth temperature for all these films was 530 °C. Details of the growth has been presented previously [14].

Plane-view (PV) and cross-sectional (CS) transmission electron microscopy examinations were carried out in a Philips CM12 operated at 120 kV. PV samples were prepared by first mechanically thinning them from substrate side to less than 100 μm. Next, samples were further thinned to electron transparency by ion milling using a 3 – 5 kV, 0.3 – 0.6 mA, Ar^+-ion beam incident at 25°, and lowered to 10° when close to finish. CS samples were prepared in the following steps. First, a diamond saw was used to cut two 2 × 4 mm cross-sectional pieces, in <011> directions, from each epi-layer sample. M-bond adhesive was used to attach the two pieces together, face to face (epi-layers). Next using M-bond adhesive glue, the two-pieces were glued onto a hollow copper grid (sometimes we glued

REPRODUCED AT GOVT EXPENSE

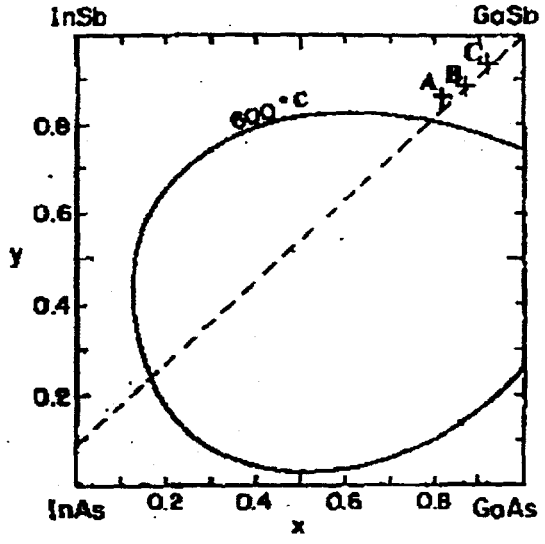

Figure 1. Phase diagram shows the relative positions of samples A, B and C. The solid curve is the calculated spinodal isotherm for $Ga_xIn_{1-x}As_ySb_{1-y}$ at temperature 600°C. Dashed line represents compositions for lattice-matched to GaSb [12].

one more piece of GaSb substrate to form a three-pieces sample disc for the reason of better supporting in the next polishing step). The subsequent thinning step is the same as plane-view sample preparation described above. HRXRD experiments were delivered by using BEDE D1 high resolution x-ray diffractometer. RSM was used to study the quality and microstructure of the sample by distinguishing between peak broadening resulting from lattice tilts and variations in lattice parameter.

EXPERIMENTAL RESULTS

Table I and Figures 2 and 3 summarize the structural changes observed by electron diffraction, associated with the varying compostions of the samples used. What is most significant in these observations is the presence of a {110} type ordering instead of the CuPt type ordering that is often reported. As discussed in our previous study [15], there have been some reports in the literature suggesting the possibility of such transformations but possible mechanisms as described in this paper have not been proposed. The electron diffraction patterns of samples D and E showed more evidence of diffuse streaking compared to those of non-misorientated samples. The diffuse scattering observed in the electron diffraction patterns of sample D and E might indicate the formation of short range ordering [16].

REPRODUCED AT GOVT EXPENSE #48

Table I: Summary of electron diffraction results of plane view samples

Sample	Variants of Diffuse Scattering	Ordering Type Reflections
A^{PV}	$[110]\&[1\bar{1}0]$	Weak (110) type reflections
B^{PV}	$[110]\&[1\bar{1}0]$	None
C^{PV}	$[110]\&[1\bar{1}0]$ $[001]\&[010]$	Weak (110) reflections
D^{PV} (same composition as A; $2°\rightarrow(110)$ on (100)	$[110]\&[1\bar{1}0]$ $[001]\&[010]$	Weak (110) reflections
E^{PV} (same composition as A; $2°\rightarrow(111_B)$ on (100)	$[110]\&[1\bar{1}0]$ $[001]\&[010]$	Weak (110) reflections

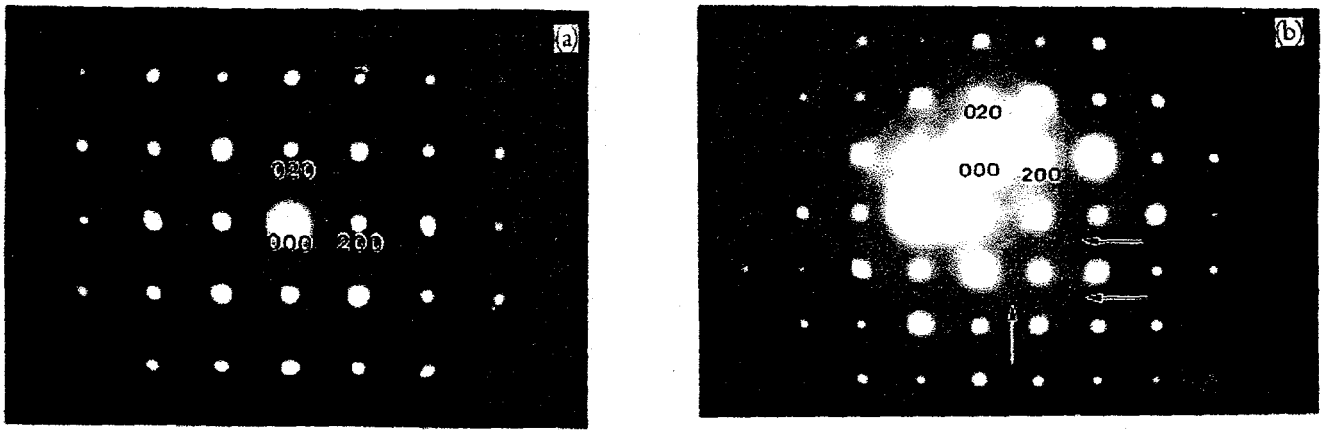

Figure 2. (a) Transmission electron microscopy (TEM) diffraction pattern of $Ga_{0.87}In_{0.13}As_{0.12}Sb_{0.88}$, sample B, showing very weak diffuse scattering in [110] and $[1\bar{1}0]$ directions. (b) TEM diffraction pattern of $Ga_{0.92}In_{0.08}As_{0.07}Sb_{0.93}$, sample C, showing strong diffuse scattering in [110] and $[1\bar{1}0]$ directions and in [100] and [010] directions with weak reflection at (110) type positions.

REPRODUCED AT GOVT EXPENSE

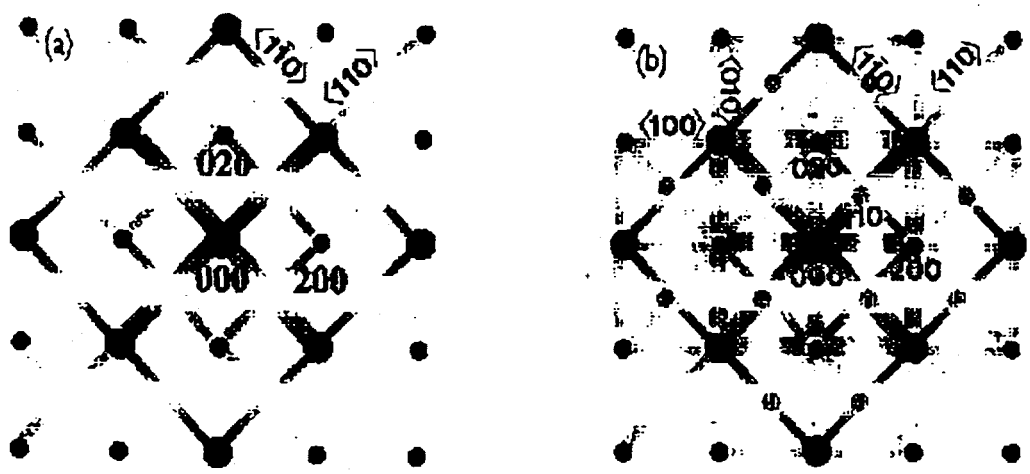

Figure 3. Schematic diagrams of the TEM diffraction patterns of (a) $Ga_{0.82}In_{0.18}As_{0.14}Sb_{0.86}$, sample A, and $Ga_{0.87}In_{0.13}As_{0.12}Sb_{0.88}$, sample B, showing weak diffuse scattering in [110] and [1 $\bar{1}$ 0] directions. (b) $Ga_{0.92}In_{0.08}As_{0.07}Sb_{0.93}$, sample C, and $Ga_{0.82}In_{0.18}As_{0.14}Sb_{0.86}$ 2° misorientated toward (110), sample D, showing strong diffuse scattering in [110] and [1 $\bar{1}$ 0] directions and in [100] and [010] directions and the evolution of weak (110) type reflection.

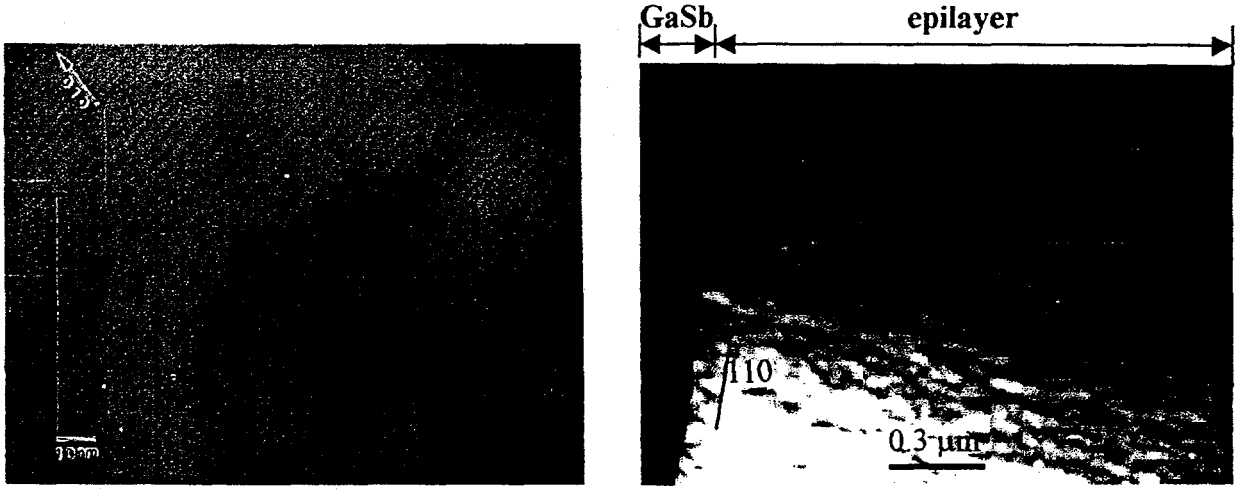

Figure 4. (a) Plane-view dark-field image, with (220) reflection, of sample C showing the weak modulation contrast near along the [010] direction. The periodicity of the modulation is about 2.6 nm. (b) Bright-field image of cross-sectional sample E^{cs}, same composition as sample A, substrate 2° misorientated toward (111_B) showing the significant effects of substrate misorientation on the stability and microstructure of the epi-layer. A fine mottled contrast with a quasi-period of 10-20 nm is distinctly observed along the [110] direction.

REPRODUCED AT GOV'T EXPENSE # 40

Figure 4(a) is a plane-view dark-field image, with (220) reflection, of sample C. It shows the weak modulation contrast close to the [010] direction. The periodicity of the modulation is about 2.6 nm. The weak modulation contrast is a common feature of plane-view samples B, C and D in the dark-field imaging study, and the results are summarized in Table II. Figure 4(b) is a bright-field image of cross-sectional sample E^{cs}, which has the same composition as sample A with a substrate 2° misorientated toward (111_B). It shows the significant effects of substrate misorientation on the phase stability and microstructure of the epi-layer. A fine mottled contrast with a quasi-period of 10-20 nm is distinctly observed along [110] direction, which was not observed on the non-misoriented samples.

Table II: Summary of dark-field imaging results

Sample	Reflection plane	Direction of Modulation	Periodicity (nm)
B^{PV}	(220)	~[110]	3.4
C^{PV}	(220)	~[110]	3.7
D^{PV}	(220)	~[010]	2.6

High resolution x-ray diffraction reciprocal space maps of (004) reflection and triple axis $\theta/2\theta$ curves for two distinct lattice matched undoped epitaxial film compositions, sample C and A were collected as shown in figures 5 and 6. It is noted that these x-ray results corroborate for both epitaxial films and support the electron diffraction results which showed a significant diffuse intensity scattering. The broad returns in the RSMs along the TH/2TH axis indicates that a significant distribution of lattice sizes exist in the epilayer. The lack of broadening in the AXIS2 direction indicates the distribution of lattice tilts is small.

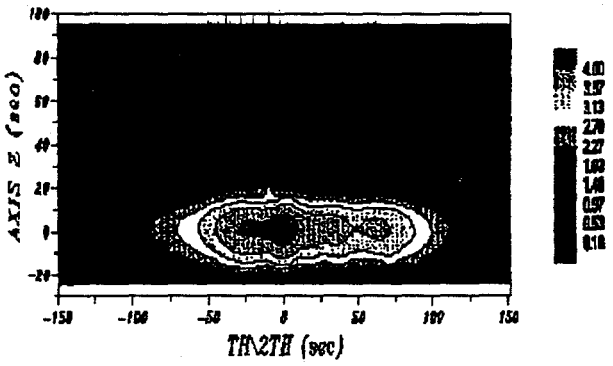

Figure 5. HRXRD reciprocal space map of sample C showing significant spread-out lattice parameter (TH/2TH) which is consistent with the weak and diffuse scattering observed in the electron diffraction pattern.

REPRODUCED AT GOVT EXPENSE #48

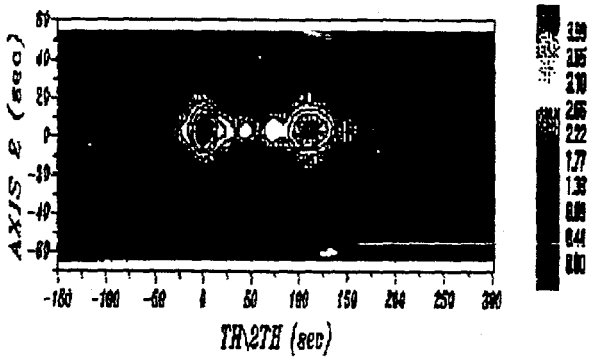

Figure 6. HRXRD reciprocal space map of sample A, showing separate peaks of GaSb substrate and epilayer and the indication of lattice parameter variations in the epilayer.

DISCUSSION

The change in crystallography of compositional modulation (Table II) and microstructures (Fig. 4(b)), with surface tilt implies that surface structure has a significant effect on the phase stability of the epitaxial layers. The study of Henoc et al. [13] on $In_{1-x}Ga_x As_yP_{1-y}$ layers, grown on (001) InP substrates by use of LPE, indicates the presence of two types of contrast modulations in TEM: fine-scale speckle microstructure and coarser scale contrast modulations with wavelengths of 10 and 125 nm, respectively. Figure 4(b), showed the same type of fine scale mottled structure with wavelength, 10-20 nm, is also similar to their results. However there was no coarse-contrast modulation as found in our study. Ahrenkiel et al. [17] found that there was the "self-organized formation of compositionally modulated ZnSeTe superlattices" with a periodicity of 1.8 – 3.2 nm when grown on a >2° tilted substrate along <111> directions. The substrate misorientation condition they used is similar to our sample E, 2° toward (111_B), and the results are consistent to those observed in Figure 4(b). The relationship between this type of composition modulation and substrate misorientation is not well established yet. However, it is believed that it is closely related to the atomic steps associated with the tilted vicinal surface.

Diffuse scattering can arise from short range order in the specimen due to either microdomains of ordered nuclei or local regions of increased order analogous to spinodal decomposition [16]. These regions produce diffuse intensity maximum at positions that will eventually correspond to a superlattice spot when the short range order has developed to long range order [18]. Combined with our electron diffraction results and fine mottled structure found in TEM bright field image, figure 4 (b), the evolution of long range order may be preceded by different stages of phase stability ranging from spinodal decomposition to short range ordering. Also the tendency of the phase instability appears to increase when epilayer composition approaches the equilibrium spinodal curve.

The high resolution x-ray diffraction results confirm that the diffuse scattering intensity observed in the electron diffraction studies are real effects that are occurring over a much larger volume of material than originally indicated when sampled by the electron diffraction. The distribution of lattice sizes observed in the HRXRD curves is an indication

REPRODUCED AT GOV'T EXPENSE # 48

of changes in the local composition (while the overall composition is lattice-matched to GaSb). This indicates that this composition is not randomly distributed. These compositional changes may be manifested in spinodal decomposition, lateral compositional modulations, short range order, and long range order covering different length scales in these structures. The implications of these changes in local composition indicates that anisotropy in properties would be expected and this has been seen in previous studies of ternary III-V compound semiconductors.

CONCLUSIONS

In this study we have shown the phase stability, microstructure and the crystallographic results for LPE grown $In_xGa_{1-x}As_ySb_{1-y}$/GaSb epitaxial layers. Our conclusion in this study include:

1. Diffuse scattering was found in <100> and <110> directions. Different crystallographic variants in compositional modulation have been observed along with the development of weak (110) ordering.
2. Composition modulation with periodicity of 2.5 – 4.0 nm was found in [110] and [010] directions in the lattice-matched epilayers.
3. Substrate misorientation has significant effect on the growth condition of the vicinal growth surface. Composition modulation due to spinodal decomposition was found in epilayer grown on 2° misoriented toward (111_B) substrate.
4. HRXRD results are consistent with the TEM studies. The spreading of lattice parameter is consistent with the diffuse scattering intensity seen in electron diffraction patterns.

REFERENCES

1. D. A. Porter and K. E. Easterling ; "Phase Transformation in Metals and Alloys" Chapman & Hall, p308, (1992)
2. O. Ueda, S. Isozumi and S. Komiya; Japanese Journal of Applied Physics **23** L241 (1984)
3. J. M. Millunchick, R. D. Twesten, S. R. Lee, D. M. follstaedt, and E. D. Jones; Journal of Electronic Materials, **26** 1048 (1997)
4. S. N. G. Chu, S. Nakahara, K. E. strege, and W. D. Johnston, Jr; Journal of Applied Physics **57** 4610 (1985)
5. S. Mahajan, B. V. Dutt, H. Temkin, R. J. Cava and W. A. Bonner; Journal of Crystal Growth **68** 589 (1984)
6. T. L. McDevitt, S. Mahajan, and D. E. Laughlin; Physical Review B **45** 6614 (1992)
7. G. C. Hua, N. Otsuka, D. C. Grillo, J. Han, L. He and R. L. Gunshor; Journal of Crystal Growth **138** 367 (1994)
8. P. Abraham, M. A. Garcia Perez, T. Benyattou, G. Guilot, M. Sacilotti, and X. Letartre; Semicond. Sci. Technol. **10** 1585 (1995)
9. S. T. Chou, K. Y. Cheng, L. J. Chou, and K. C. Hseih, Journal of Applied Physics **78** 6270 (1995)
10. A. C. Chen, A. M. Moy, L. J. Chou, K. C. Hsieh, and K. Y. Cheng; Applied Physics Letters **66** 2694 (1995)

REPRODUCED AT GOVT EXPENSE

11. F. Peiro, A. Cornet, J. C. Ferrer, J. R. Merante, G. Halkias, and A. Georgakilas; Materials Research Society Symposium Proceedings, edited by E. D. Jones, A. Mascarenhas, and P. Petroff (MRS, Pittsburgh, 1996) p265
12. K. Onabe; Japanese Journal of Applied Physics **21** 964 (1982)
13. P. Henoc, A. Izrael, M. Quillec and H. Launois; Appl.Phys Lett. **40** 963 (1982)
14. J. C. DeWinter, M. A. Pollack, A. K. Srivastava, and J. L. Zyskind; Journal of Electronic Materials, **14** 729 (1985)
15. Y-C. Chen, V. Bucklen, M. Freeman, R. P. Cardines Jr, and K. Rajan; 40th Electronic Materials Conference (1998)
16. D. B. Williams and C. B. Carter; "Transmission Electron Microscopy" II, Plenum Press, New York, p259 (1996)
17. S. P. Ahrenkiel, S. H. Xin, P. M. Reimer, J. J. Berry, H. Luo, S. Short, M. Bode, M. Al-Jassim, J. R. Buschert, and J. K. Furdyna; Physical Review Letters **75** 1586 (1995)
18. J. M. Cowley; Acta Crystallographica **A29** 529 (1973)